第 35 卷第 6 期 无 机 化 学 学 报 Vol.35 No.6
2019 年 6 月 CHINESE JOURNAL OF INORGANIC CHEMISTRY 1101-1108

尖晶石结构 MFe_2O_4(M=Ca,Mg,Cu,Zn)纳米晶粉末的制备和磁性能

陈 鹏[1] 姜林文*,[1] 刘进军[1] 杨姗姗[1] 李江涛[1] 陈红兵[1] 何 骏*,[2] 王 煜[2]
([1]宁波大学材料科学与化学工程学院,新型功能材料及其制备科学国家重点实验室培育基地,宁波 315211)
([2]钢铁研究总院功能材料研究所,北京 100081)

摘要:采用新型氨基凝胶自燃法成功制备出尖晶石结构 MFe_2O_4(M=Ca,Mg,Cu,Zn)纳米晶粉末。对合成粉体样品的物相、形貌和磁性能进行了详细的研究。经能量色散 X 射线谱分析确定了合成 MFe_2O_4 粉末的高纯度。系统地研究了所合成的 MFe_2O_4 纳米晶粉末的磁性能。所有样品的磁滞回线均较窄,表明了它们具有软磁的特征。经测试得出 4 种铁氧体的饱和磁化强度(M_s)分别为 2.1,29.3,24.1 和 4.2 emu·g^{-1};剩余磁化强度(M_r)分别为 0.2,2.3,11.4 和 0.2 emu·g^{-1}。这 4 种铁氧体样品的 M_r/M_s 值均小于 0.5。对 $CaFe_2O_4$ 和 $MgFe_2O_4$ 两种典型铁氧体的零场冷却和场冷磁性能作了详细的研究。其中 $CaFe_2O_4$ 样品的磁化强度在 75 K 以下有不一致的变化趋势,这是由于其发生了磁相变。

关键词:尖晶石型铁氧体;自燃烧法;磁性能
中图分类号:O482.54 **文献标识码**:A **文章编号**:1001-4861(2019)06-1101-08
DOI:10.11862/CJIC.2019.133

Syntheses and Magnetic Properties of Spinel-Type MFe_2O_4 (M=Ca, Mg, Cu, Zn) Nanocrystalline Powders

CHEN Peng[1] JIANG Lin-Wen*,[1] LIU Jin-Jun[1] YANG Shan-Shan[1]
LI Jiang-Tao[1] CHEN Hong-Bing[1] HE Jun*,[2] WANG Yu[2]
([1]*State Key Laboratory Base of Functional Materials and its Preparation Science, Key Laboratory of Photoelectric Detection Materials and Devices of Zhejiang Province, Ningbo University, Ningbo, Zhejiang* 315211, *China*)
([2]*Division of Functional Material Research, Central Iron & Steel Research Institute, Beijing* 100081, *China*)

Abstract: Magnetic spinel-type MFe_2O_4 (M=Ca, Mg, Cu and Zn) nanocrystalline powders were successfully prepared by auto-combustion method using a novel amino-based gel. The phase identification, morphology and magnetic properties of as-synthesized powders were studied in detail. The high purity of synthesized MFe_2O_4 powders was comfirmed by energy dispersive X-ray spectroscopy. Magnetic properties of as-synthesized MFe_2O_4 nanocrystalline powders were investigated systematically. All the samples presented a rather narrow hysteresis loop, suggesting the soft magnetic features. The saturated magnetization (M_s) of the four ferrites were 2.1, 29.3, 24.1, and 4.2 emu·g^{-1}, respectively, and the residual magnetization (M_r) were 0.2, 2.3, 11.4, and 0.2 emu·g^{-1}, respectively. M_r/M_s values of four ferrite samples were all less than 0.5. Zero-field-cooled and field-cooled magnetic properties of $CaFe_2O_4$ and $MgFe_2O_4$ samples as two typical ferrites were investigated in detail. The magnetization of $CaFe_2O_4$ sample presented an inconsistent variation tendency below 75 K due to the occurrence of magnetic phase transition.

Keywords: spinel-type ferrites; auto-combustion method; magnetic properties

收稿日期:2019-01-06。收修改稿日期:2019-03-30。
国家自然科学基金(No.51701098)、宁波市自然科学基金(No.2017A610100)、山东大学晶体材料国家重点实验室开放项目(No.KF1706)和宁波大学王宽城幸福基金项目资助。
*通信联系人。E-mail:jianglinwen@nbu.edu.cn,hejun@cisri.com.cn

0 Introduction

Recently, magnetic spinel-type ferrites have been investigated extensively for their excellent properties and broad applications[1-10]. Spinel-type ferrites with a formula of MFe_2O_4 and a structure of cubic unit cell can be found in a broad range of applications, such as transformer cores, high density storage, biomedical fields like hyperthermia of cancer treatment, targeted drug delivery[11-13]. As is known to all, calcium ferrite ($CaFe_2O_4$) magnetic nanoparticles have the features of monodispersity, stability, superparamagnetism, and biocompatibility[14-15]. Besides, $CaFe_2O_4$ is biocompatible and eco-friendly owing to the presence of Ca^{2+} instead of heavy metals[16]. Magnesium ferrite ($MgFe_2O_4$) is a magnetic bi-oxide ceramic material, which possesses the excellent chemical stability and partial inverse spinel structured $(Mg_{1-\delta}Fe_\delta)[Mg_\delta Fe_{2-\delta}]O_4$, where δ stands for the degree of inversion of cation in the structure[17-18]. $MgFe_2O_4$ can be used in the fields of treating tumors using a thermal coagulation technique[19], catalysis[20], gas sensors[21], as well as the fuel cell cathode for molten electrolytes due to the enhancement of the stability and performance[22]. Copper ferrite ($CuFe_2O_4$) is one of the most important spinel-type ferrites, which has the structural phase transformation and the reduction of the crystal symmetry known as Jahn-Teller distortion[23]. In addition, the magnetic properties of $CuFe_2O_4$ are strongly determined by the Cu ions, especially in the nano-scale size when the magnetic domain size is smaller than the grain boundaries[24]. Zinc ferrite ($ZnFe_2O_4$) also has the partially inverted spinel structure of $(Zn_{1-\delta}Fe_\delta)[Zn_\delta Fe_{2-\delta}]O_4$ like $MgFe_2O_4$, and it also possesses rather good magnetic and electrical properties[25]. Furthermore, $ZnFe_2O_4$ is a potential material to be widely in the applications of gas sensor, semiconducting photocatalysis, magnetic resonance imaging, drug-delivery, light-driven water-splitting, ferrofluid, magnetic data storage, etc[26-29].

At present, $CaFe_2O_4$ have been investigated by some researchers. Sulaiman et al. reported that $CaFe_2O_4$ nanoparticles synthesized by co-precipitation method have much larger saturation magnetization than those fabricated by auto-combustion method[30]. Manohar et al. studied the room-temperature magnetic properties of $CaFe_2O_4$ nanocrystals prepared by solvothermal reflux method[31]. However, Zhang et al. have synthesized $CaFe_2O_4$ nanocrystal by solution combustion, which could be used as a magnetically separable photocatalyst[32]. Da Dalt et al. studied magnetic and Mssbauer behavior of the nanostructured $MgFe_2O_4$ spinel ferrite obtained at low temperature[33]. Inaddition, Druc et al. invstigated magnetic and dielectric properties for $MgFe_2O_4$ ferrite at room temperature[34]. However, there are very few reports about the studies of zero-field-cooled (ZFC) and field-cooled (FC) magnetic properties of $CaFe_2O_4$ and $MgFe_2O_4$ ferrites.

In this study, MFe_2O_4 (M=Ca, Mg, Cu and Zn) nanocrystalline powders were synthesized by auto-combustion method using a novel amino-based gel. ZFC and FC magnetic properties of $CaFe_2O_4$ and $MgFe_2O_4$ nanocrystalline were specially investigated in this work. The results showed that $CaFe_2O_4$ exhibits a magnetic phase transition of antiferromagnetic state to paramagnetic state below 75 K, which would help us to better understand the mechanism of low-temperature magnetic phase transition. In addition, $MgFe_2O_4$ nanocrystalline sample has a superparamagnetic behavior, making the ferrite promising for magnetic recording application.

1 Experimental

1.1 Materials

$Ca(NO_3)_2\cdot 4H_2O$ (98.5%), $Mg(NO_3)_2\cdot 6H_2O$ (98.5%), $Cu(NO_3)_2\cdot 3H_2O$ (98.5%), $Zn(NO_3)_2\cdot 6H_2O$ (98.5%), $Fe(NO_3)_3\cdot 9H_2O$ (98.5%), and alanine ($C_3H_7NO_2$, AR) were all purchased from the Sinopharm Chemical Reagent Corporation (Shanghai China).

1.2 Synthesis of MFe_2O_4 nanocrystalline powders

A series of spinel-type ferrites of MFe_2O_4 (M=Ca, Mg, Cu and Zn) were synthesized by sol-gel auto-combustion method. The flowchart presenting the method of preparation is detailedly exhibited in Fig.1.

Calcium nitrate [$Ca(NO_3)_2 \cdot 4H_2O$], magnesium nitrate [$Mg(NO_3)_2 \cdot 6H_2O$], copper nitrate [$Cu(NO_3)_2 \cdot 3H_2O$], zinc nitrate [$Zn(NO_3)_2 \cdot 6H_2O$], and ferric nitrate [$Fe(NO_3)_3 \cdot 9H_2O$] were used as the precursors, while alanine ($C_3H_7NO_2$) was acted as the combustion agent for the auto-combustion process. $M(NO_3)_2$ (M=Ca, Mg, Cu and Zn) and $Fe(NO_3)_3 \cdot 9H_2O$ with an accurate stoichiometric ratio of n_M:n_{Fe}=1:2 were dissolved in the distilled water by stirring vigorously. The alanine was added into above solution, and the molar ratio of alanine to metal ions was set at 1:1. Subsequently, the mixture was stirred and heated continuously until the mixture was almost evaporated dried and the sticky gel was formed. Then the sticky gel was transferred into an open alumina crucible, and the gel was burned by an auto-propagating manner. In this typical synthesis process, magnetic nanocrystalline powders were obtained successfully. Finally, all of as-obtained nanocrystalline powders were annealed at different temperatures for 2 h in a muffle furnace.

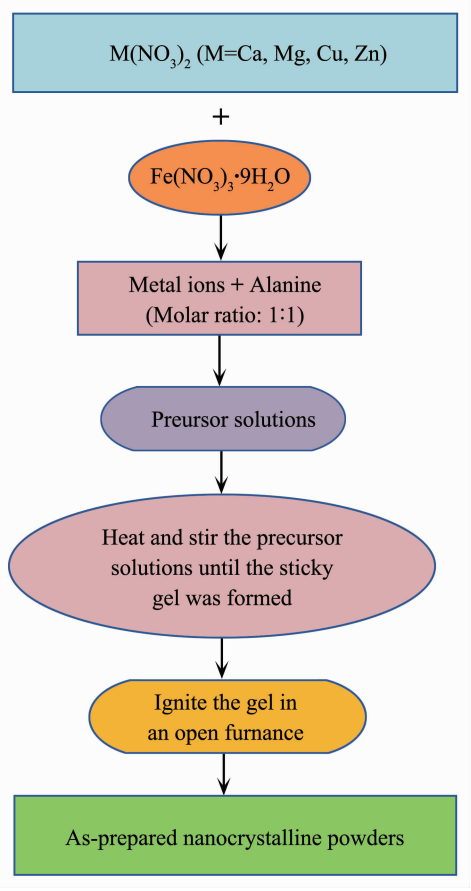

Fig.1　Flowchart of preparing MFe_2O_4 (M=Ca, Mg, Cu and Zn) nanocrystalline powders by sol-gel auto-combustion method

1.3　Sample characterization

The phase identification of MFe_2O_4 nanocrystalline powders was confirmed using a Bruker D8 diffractometer with Cu $K\alpha$ radiation (λ=0.154 06 nm, U=40 kV, I=40 mA) at a scan rate of 8°·min^{-1} from 10° to 80° (2θ). The morphologies of the samples were characterized by a scanning electron microscope with 20 kV operating voltage, which was equipped an energy dispersive X-ray spectroscopy (EDS) analyzer (SEM, SU-70, Hitachi, Japan). The magnetic properties of the samples were investigated by a vibrating sample magnetometer (VSM Lakeshore-7410, America).

2　Results and discussion

2.1　X-ray analysis

The phase structures of the as-prepared MFe_2O_4 (M =Ca, Mg, Cu and Zn) nanocrystalline powders annealed at 900 ℃ were investigated by X-ray diffraction (XRD), as shown in Fig.2(a). The XRD patterns of four as-prepared nanocrystalline powders are all well in accordance with their standard cards, suggesting that the pure phase of nanocrystalline powders had been obtained successfully. However, there are residual organic compounds in the as-burnt nanocrystalline powders. Therefore, the as-burnt samples should be annealed. Fig.2(b) exhibits the XRD patterns of $CaFe_2O_4$ powders annealed at the temperature of 600, 700, 800, 900, 1000, 1 100 and 1 200 ℃, respectively. In Fig.2(b), the diffraction peaks of as-burnt $CaFe_2O_4$ nanocrystalline exactly corresponded to the PDF#65-1333 until the annealed temperature is 700 ℃, suggesting that residual organic compounds in as-burnt $CaFe_2O_4$ powders can be removed when the temperature is above 700 ℃. In addition, according to our previous work[35], the residual organic compounds in as-burnt $GdFeO_3$ powders prepared by sol-gel auto-combustion method can be removed by annealing at 800 ℃. Therefore, in order to ensure the removal of organic matter from the as-burnt powders, all of the samples for characterization were annealed at temperature of 900 ℃.

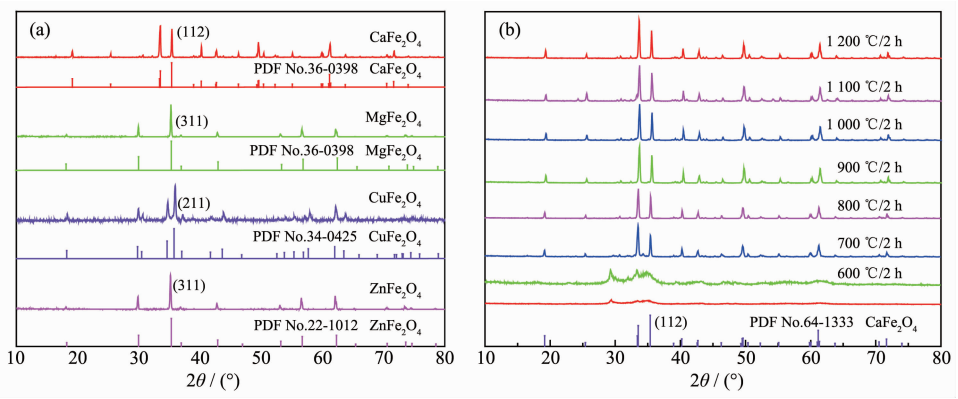

Fig.2 XRD patterns of four spinel-type ferrite nanocrystalline powders annealed at 900 ℃ (a) and as-prepared $CaFe_2O_4$ powders annealed at different temperatures (b)

2.2 Microstructure analysis

Typical SEM micrographs of four kinds of as-prepared nanocrystalline powders annealed at 900 ℃ are well performed in Fig.3(a~h), respectively. In Fig.3(a,b), it can be seen that as-obtained $CaFe_2O_4$ nanocrystalline powders were spongy and porous agglomerating with many pores, which were induced by the instantaneously-released gases during the auto-combustion process. Fig.3(c,d) show the microscopic morphology of as-prepared $MgFe_2O_4$ nanocrystalline powders, and it can be observed that the $MgFe_2O_4$ powders presented sponge-like shape with lots of tiny bubbles. Fig.3(e,f) exhibit the micrograph of $CuFe_2O_4$ nanocrystalline powders, and it can be seen that there were plenty of pores presented in the sample. In Fig.3(g), we can observe that $ZnFe_2O_4$ powders were spongy and porous in morphology, and a high-magnification SEM image shown in Fig.3(h) clearly revealed that as-synthesized $ZnFe_2O_4$ nanocrystalline powders were spherical. Totally speaking, all of as-prepared powders have the porous and spongy morphology with plenty of pores. The pores could reduce the interactions between nanocrystalline powders, as well as be beneficial to magnetic materials.

2.3 EDS spectra analysis

As known to us all, magnetic properties of powders are sensitive to the constitutive components, such as Fe_2O_3, CaO, MgO, CuO, ZnO. The undesired matters may appear during the auto-combustion process owing to the drastic and uncontrollable reaction, which would seriously influence the results

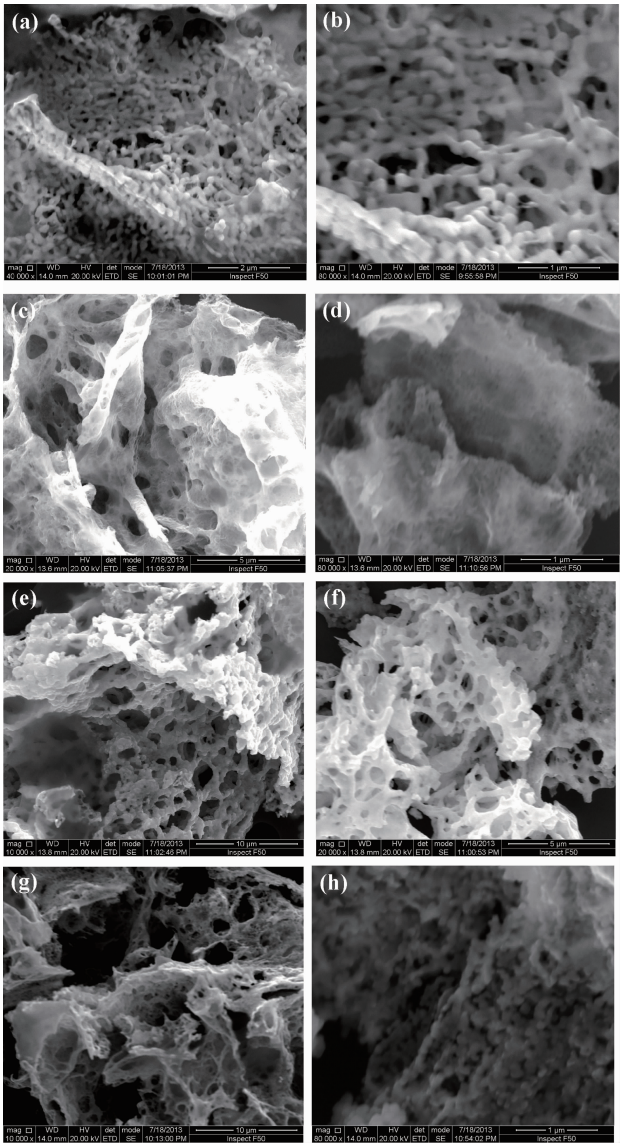

Fig.3 SEM images of $CaFe_2O_4$ (a, b), $MgFe_2O_4$ (c, d), $CuFe_2O_4$ (e, f) and $ZnFe_2O_4$ (g, h) powders annealed at 900 ℃

of intrinsic magnetic properties of the samples. In order to investigate the purity of as-synthesized powders, the EDS technique was used to measure the molar ratios of atoms in the samples. Fig.4(a~d) show the EDS spectra of as-obtained magnetic nanocrystalline powders: $CaFe_2O_4$, $MgFe_2O_4$, $CuFe_2O_4$ and $ZnFe_2O_4$, respectively. It can be seen that the ratios of n_M:n_{Fe} (M=Ca, Mg, Cu and Zn) are all close to the theoretical value of 1∶2. However, according to the statistical data in Table 1, we can know that the contents of O element of all the samples are obviously higher than the theoretical values. The much higher content of O element may be caused by the residual organic matters with oxygen element, which could enhance the content of detected oxygen[36].

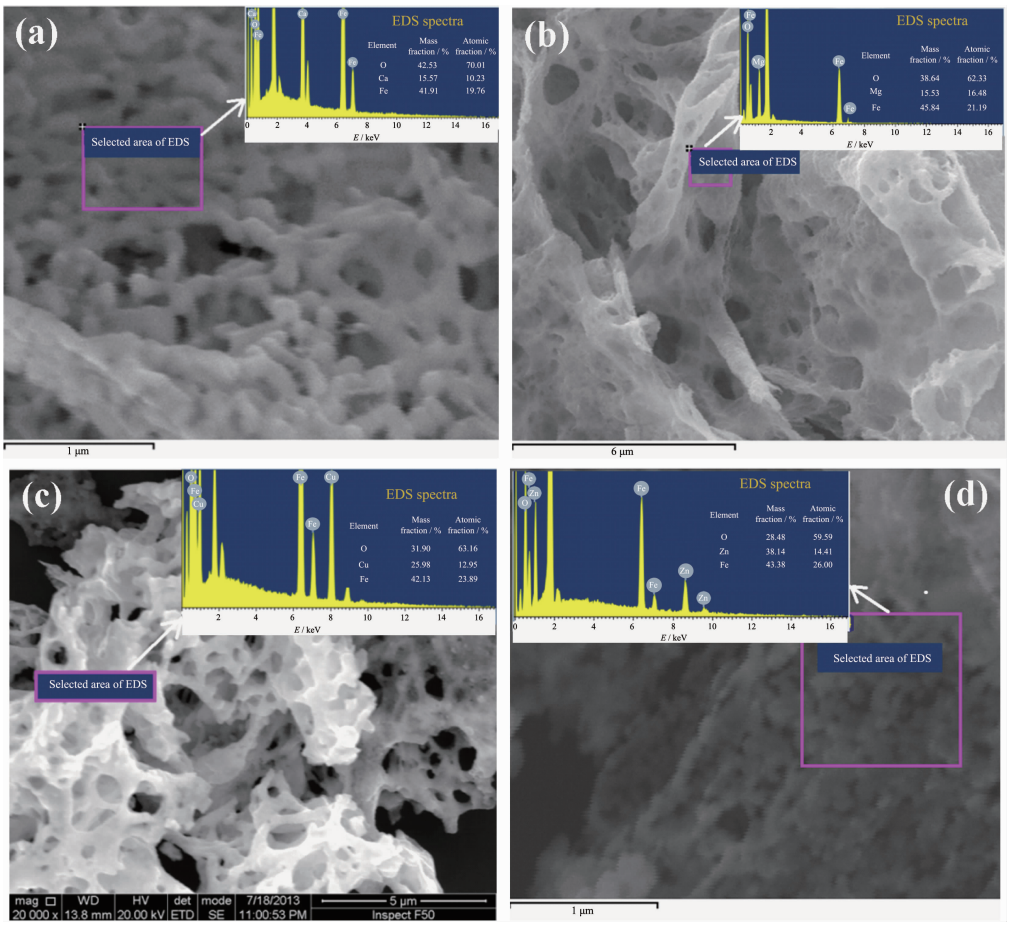

Fig.4　EDS spectra of as-synthesized nanocrystalline powders: (a) $CaFe_2O_4$; (b) $MgFe_2O_4$; (c) $CuFe_2O_4$; (d) $ZnFe_2O_4$

Table 1　Comparison of theoretical and measured values of element contents of as-prepared samples

Sample	$CaFe_2O_4$			$MgFe_2O_4$			$CuFe_2O_4$			$ZnFe_2O_4$		
Constituent element	O	Ca	Fe	O	Mg	Fe	O	Cu	Fe	O	Zn	Fe
Measured mass fraction / %	42.5	15.6	41.9	38.6	15.3	45.8	31.9	26.0	42.1	28.5	38.1	43.4
Theoretical mass fraction / %	29.6	18.5	51.9	32.0	12.0	56.0	26.7	26.7	46.7	25.6	27.0	46.5

2.4　Magnetic properties

Magnetic properties of the ferrite nanocrystalline powders are significant for their application in magnetic recording, magneto-optical recording, as well as other electronic devices. The hysteresis loops of as-prepared MFe_2O_4 (M=Ca, Mg, Cu and Zn) nanocrystalline powders measured using a vibrating sample magnetometer (VSM) at room temperature are exhibited in Fig.5(a~d). From Fig.5, it can be observed that all the samples presented a rather narrow hysteresis loop, suggesting a behavioral characteristic of soft magnetic features[34]. The related hysteresis parameters of as-

prepared samples are concretely described in the Table 2. From the hysteresis loops, it can be observed that $CaFe_2O_4$ and $ZnFe_2O_4$ powders have rather low saturation magnetization (M_s) and residual magnetization (M_r). Whereas, $MgFe_2O_4$ and $CuFe_2O_4$ powders have rather large M_s and M_r values, which may be induced by their larger particle sizes. According to the references[37-39], the saturation magnetization (M_s) increases with the increase in particle size. In Fig.4(a~d), it can be observed that $CuFe_2O_4$ powders have the largest coercive force (H_c) value in the four kinds of nanocrystalline powders. As we all know, H_c is different from M_s and M_r, since particle size is not a unique factor determining H_c. H_c is determined by some complex factors, such as microstructure, particle/grain size, residual strain[40-41]. Besides, Table 2 also exhibited the values of loop squareness ratios, M_r/M_s. In Table 2, it can be found that all of the calculated M_r/M_s values were less than 0.5, indicating the particles could interact by magnetostatic interactions [42]. According to the given values, it is quite possible for these materials to be used in the field of cores and coils with low inductance[43].

To investigate the detailed magnetic behaviors, $CaFe_2O_4$ and $MgFe_2O_4$ as two typical ferrites were employed to determine ZFC and FC properties. Fig.6 (a,b) display the ZFC and FC magnetization curves for the two nanocrystalline samples of $CaFe_2O_4$ and $MgFe_2O_4$, respectively. In Fig.6(a), the ZFC process of $CaFe_2O_4$ had a sharp increase from 0 (5 K) to 0.20 emu·g^{-1} (75 K), and a slow increase from 0.20 emu·g^{-1} (75 K) to 0.24 emu·g^{-1} (300 K). In the ZFC process, temperature plays a crucial role in determing the magnetization due to the absence of applied field.

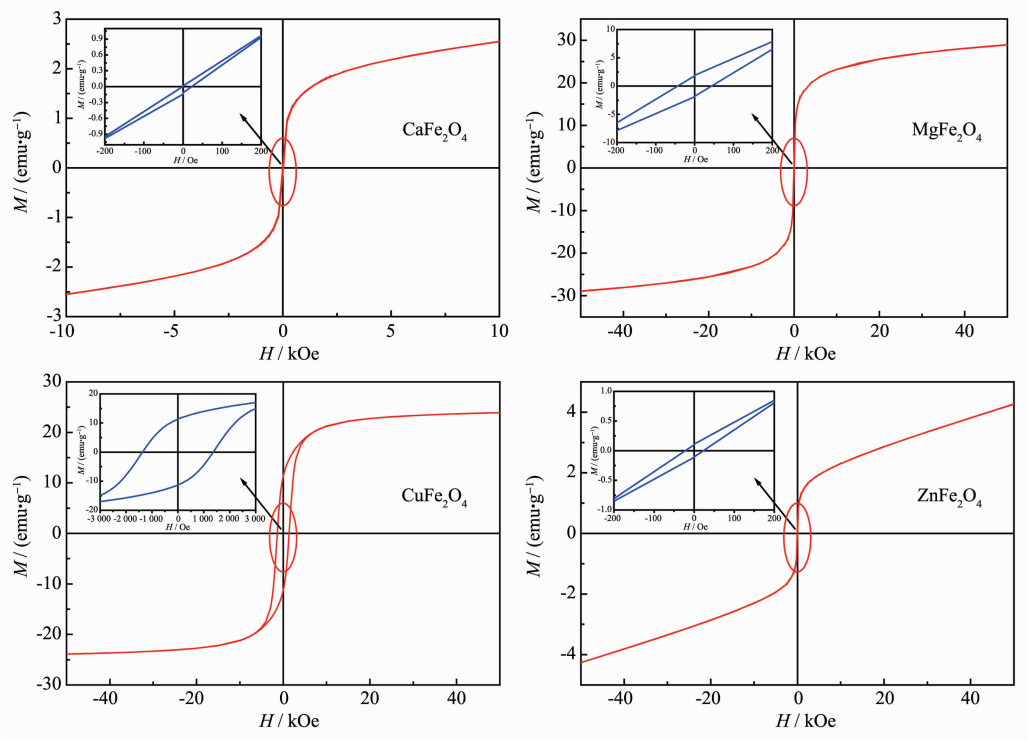

Fig.5 Hysteresis loops of $CaFe_2O_4$ (a), $MgFe_2O_4$ (b), $CuFe_2O_4$ (c) and $ZnFe_2O_4$ (d) powders

Table 2 Hysteresis parameters of as-prepared samples at the room temperature

Sample	Field / kOe	M_s / (emu·g^{-1})	M_r / (emu·g^{-1})	H_c / Oe	M_r / M_s
$CaFe_2O_4$	10	2.1	0.2	25	0.095
$MgFe_2O_4$	50	29.3	2.3	49	0.078
$CuFe_2O_4$	50	24.1	11.4	1 375	0.473
$ZnFe_2O_4$	50	4.2	0.2	28	0.048

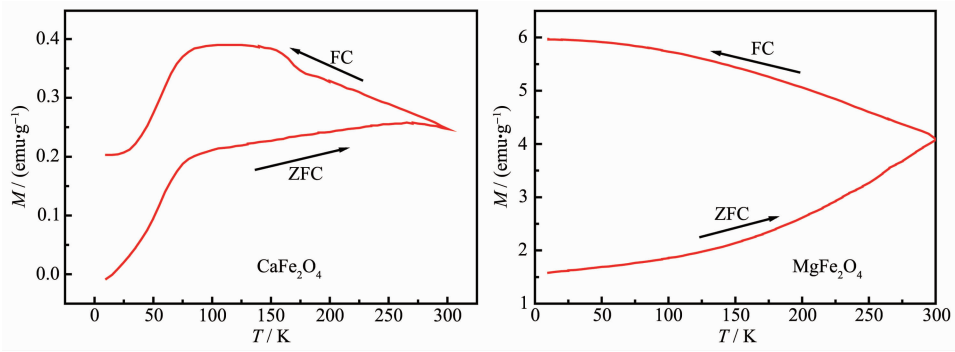

Fig.6　Temperature dependence of the magnetization in ZFC and FC for $CaFe_2O_4$ (a) and $MgFe_2O_4$ (b) powders

In this case, the high temperature can provide the related thermal disturbance, and cause the oriented rotation of magnetic domain, so the magnetization presents an obvious increase with the temperature increasing. When the sample was cooled from 300 K to 5 K (FC), the magnetization of $CaFe_2O_4$ increased from 0.24 emu·g^{-1} (300 K) to 0.38 emu·g^{-1} (75 K), while decreased from 0.38 emu·g^{-1} (75 K) to 0.24 emu·g^{-1} (5 K). In contrast, in the FC process, the magnetization increased with the temperature decreasing in the condition of adding an applied field. It might be due to that the thermal disturbance has the random orientation, which can weaken the effect of applied field on the magnetization of sample. As in the reference[44], the magnetization of $CaFe_2O_4$ is initially constant as the temperature is decreased. Further lowering the temperature, magnetization increases sharply, reaches a maximum value and then decreases almost linearly down to 30 K. This behavior is typical of an antiferromagnetic material exhibiting a transition to paramagnetic state. Therefore, it can be observed a similar behavior in Fig.6(a) that the magnetization presented an inconsistent variation tendency below 75 K, which may be due to the magnetic phase transition of $CaFe_2O_4$ sample. For the sample of $MgFe_2O_4$, it can be seen from Fig.6(b) that the ZFC magnetization monotonically increased from 1.61 emu·g^{-1} (5 K) to 4.18 emu·g^{-1} (300 K). Similar with the $CaFe_2O_4$ sample, temperature plays a crucial role in determining the magnetization during the ZFC process. For the FC process, magnetization monotonically increased with the decrease of temperature from 4.18 emu·g^{-1} (300 K) to 5.95 emu·g^{-1} (5 K). Similar with the $CaFe_2O_4$ sample, the decreased magnetization might be due to the thermal disturbance that weaken the effect of applied field on the magnetization of sample. In addition, the separated ZFC and FC magnetization curves in Fig.6(b) indicate that the $MgFe_2O_4$ sample has a superparamagnetic behavior.

3　Conclusions

Auto -combustion method was applied in the preparation of spinel-type ferrites nanocrystalline powders MFe_2O_4 (M=Ca, Mg, Cu and Zn) in this work. The high purity of synthesized MFe_2O_4 powders were certified by the fact that the ratios of n_M:n_{Fe} was close to the theoretical value of 1:2 measured via an energy dispersive X-ray spectroscopy. The measured results obtained from the magnetic hysteresis loops indicated that all of the four samples have the moderate magnetism and the behavioral characteristic of soft magnetic features. $CaFe_2O_4$ presents an inconsistent variation tendency below 75 K, which is caused by a magnetic phase transition of antiferromagnetic state to paramagnetic state below 75 K. The separated ZFC and FC magnetization curves indicate that the $MgFe_2O_4$ sample has a superparamagnetic behavior.

Acknowledgements: This work is supported by Natural Science Foundation of China (Grant No.51701098), and Natural Science Foundation of Ningbo municipality (Grant No. 2017A610100). This work is also sponsored by the Opening Project of State Key laboratory of Crystal Material in Shandong University (Grant No.KF1706), and K. C. Wong Magna Foundation in Ningbo University.

Conflict of Interest: The authors declare that they have no

conflict of interest.

References:

[1] Pardeshi S K, Pawar R Y. *Mater. Res. Bull.*, **2010**,**45**(5):609-615

[2] Ida S, Yamada K, Matsunaga T, et al. *J. Am. Chem. Soc.*, **2010**,**132**(49):17343-17345

[3] Dohnalova Z, Sulcova P, Trojan M. *Dyes Pigm.*, **2009**,**80**(1):22-25

[4] Sato K, Watanabe Y, Horiuchi A, et al. *J. Surg. Res.*, **2008**, **146**(1):110-116

[5] Jiang J Z, Goya G F, Rechenberg H R. *J. Phys.*: *Condens. Mater.*, **1999**,**11**:4063-4078

[6] Pandya P B, Joshi H H, Kulkarni R G. *J. Mater. Sci. Lett.*, **1991**,**10**(8):474-476

[7] Phumying S, Labuayai S, Swatsitang E, et al. *Mater. Res. Bull.*, **2013**,**48**(6):2060-2065

[8] Tong G X, Du F F, Xiang L J, et al. *Nanoscale*, **2014**,**6**(2):778-787

[9] WANG Qing-Cheng(王清成), FU Hua(付华), ZHUANG Jia(庄稼). *Chinese J. Inorg. Chem.*(无机化学学报), **2005**,**21**(8):1223-1226

[10]FEI Peng(费鹏), FANG Yan(方燕), SU Bi-Tao(苏碧桃), et al. *Chinese J. Inorg. Chem.*(无机化学学报), **2011**,**27**(7):1329-1333

[11]Bhosale R R, Shende R V, Puszynski J A. *Int. J. Hydrogen Energy*, **2012**,**37**(3):2924-2934

[12]Stergiou C. *J. Magn. Magn. Mater.*, **2017**,**426**:629-635

[13]Sadiq I, Naseem S, Ashiq M N, et al. *Prog. Nat. Sci. Mater.*, **2015**,**25**(5):419-424

[14]Arruebo M, Fernández-Pacheco R, Ibarra M R, et al. *Nano Today*, **2007**,**2**(3):22-32

[15]MA Fu(马富), ZHAO Hong-Jian(赵红建). *Inorganic Chemicals Industry*(无机盐工业), **2018**,**50**(11):67-71

[16]Khanna L, Verma N K. *J. Magn. Magn. Mater.*, **2013**,**336**:1-7

[17]Mathew D S, Juang R S. *Chem. Eng. J.*, **2007**,**129**(1/2/3):51-65

[18]Wang Z W, Lazor P, Saxena S K, et al. *Mater. Res. Bull.*, **2002**,**37**(9):1589-1602

[19]Konishi K, Maehara T, Kamimori T, et al. *J. Magn. Magn. Mater.*, **2004**,**272**:2428-2429

[20]Jia C J, Liu Y, Schwickardi M, et al. *Appl. Catal. A*: *Gen.*, **2010**,**386**(1/2):94-100

[21]Liu Y L, Liu Z M, Yang Y, et al. *Sens. Actuators A*, **2005**, **107**(2):600-604

[22]Okawa H, Lee J H, Hotta T, et al. *J. Power Sources*, **2004**, **131**(1/2):251-255

[23]Hoque S M, Choudhury M A, Islam M F. *J. Magn. Magn. Mater.*, **2002**,**251**(3):292-303

[24]Abdellatif M H, Innocenti C, Liakos I, et al. *J. Magn. Magn. Mater.*, **2017**,**424**:402-409

[25]Yadav R S, Kuritka I, Vilcakova J, et al. *J. Phys. Chem. Solids*, **2017**,**110**:87-99

[26]Hufnagel A G, Peters K, Müller A, et al. *Adv. Funct. Mater.*, **2016**,**26**(25):4435-4443

[27]Cao Y L, Qin H Y, Niu X J, et al. *Ceram. Int.*, **2016**,**42**(9):10697-10703

[28]Chakraborty M, Thangavel R, Biswas A, et al. *CrystEngComm*, **2016**,**18**(17):3095-3103

[29]Hoque S M, Hossain M S, Choudhury S, et al. *Mater. Lett.*, **2016**,**162**:60-63

[30]Sulaiman N H, Ghazali M J, Yunas J, et al. *Ceram. Int.*, **2018**,**44**(1):46-50

[31]Manohar A, Krishnamoorthi C. *J. Alloys Compd.*, **2017**,**722**:818-827

[32]Zhang Z J, Wang W Z. *Mater. Lett.*, **2014**,**133**:212-215

[33]Da Dalt S, Takimi A S, Volkmer T M. *Powder Technol.*, **2011**,**210**(2):103-108

[34]Druc A C, Dumitrescu A M, Borhan A I, et al. *Cent. Eur. J. Chem.*, **2013**,**11**(8):1330-1342

[35]Jiang L W, Yang S S, Zheng M Y, et al. *Mater. Res. Bull.*, **2018**,**104**:92-96

[36]Jiang L W, Yang S S, Zheng M Y, et al. *Mater. Res. Express*, **2017**,**4**(12):126102

[37]Sai R, Kulkarni S D, Vinoy K J, et al. *J. Mater. Chem.*, **2012**,**22**(5):2149-2156

[38]Mendonca E C, Jesus C B R, Folly W S D, et al. *J. Appl. Phys.*, **2012**,**111**(5):053917

[39]Oliver S A, Willey R J, Hamdeh H H, et al. *Scr. Metall. Mater.*, **1995**,**33**(10/11):1695-1701

[40]Xiao S H, Jiang W F, Li L Y et al. *Mater. Chem. Phys.*, **2007**,**106**(1):82-87

[41]Ju Y W, Park J H, Jung H R, et al. *Mater. Sci. Eng. B*, **2008**,**147**(1):7-12

[42]Patil S H, Patil S I, Kadam S M, et al. *Bull. Mater. Sci.*, **1991**,**14**(5):1225-1230

[43]Ghatage A K, Choudhary S C, Patil S A. *J. Mater. Sci. Lett.*, **1996**,**15**(17):1548-1550

[44]Das A K, Govindraraj R, Srinivasan A. *J. Magn. Magn. Mater.*, **2018**,**451**:526-531